THE ELECTRICAL RESPONSE TO LIGHT OF BACTERIORHODOPSIN IN PLANAR MEMBRANES

TOM R. HERRMANN AND GEORGE W. RAYFIELD, *Physics Department, University of Oregon, Eugene, Oregon 97403 U.S.A.*

ABSTRACT We have measured the light-induced short-circuit current generated by a planar membrane containing bacteriorhodopsin incorporated by vesicle fusion. The experimental results are consistent with an equivalent electrical circuit analogue that assumes that the vesicles remain intact after fusion and that the current generator equivalent of the light-driven proton pump is linearly dependent on bias voltage.

The transient response to light of the planar membrane has also been examined. Slow response times are seen to be associated with the capacitive charging and discharging of the fused vesicles. A study of the leading edge of the light response curve of the planar membrane yields information about the transient response of the light-driven proton pump. We propose that the translocation of protons across the membrane is associated with a first-order process characterized by a rate constant λ.

INTRODUCTION

Purple membrane derived from *Halobacterium halobium* contains a single protein, bacteriorhodopsin, as well as lipids and is part of a photophosphorylating system (1, 2). The protein, bacteriorhodopsin, functions as a light-driven proton pump (3, 4). The cyclic changes in the absorption spectra of the chromophore after a light flash have been studied extensively (5–8). Indicator dyes have been used to measure the kinetics of the light-induced proton release and uptake by purple membrane (6, 7, 9).

One of the several methods which have been used to incorporate bacteriorhodopsin into a bimolecular lipid membrane (BLM)[1] involves the fusion of vesicles containing purple membrane with the BLM (10, 11). This method has several possible advantages: Since the purple membrane sheets are oriented in the vesicles (9) (protons are pumped inward under illumination), there is reason to believe that the purple membrane sheets will also be oriented when incorporated into a BLM. The method of vesicle fusion to incorporate bacteriorhodopsin into a BLM can be used quite generally to incorporate other membrane proteins into planar membranes. The membrane proteins do not need to be exposed to a hydrocarbon solvent (i.e. decane) environment. The electrical characteristics of the BLM can be measured before and after the addition of the bacteriorhodopsin.

[1] *Abbreviations used in this paper:* BLM, bimolecular lipid membrane; CCCP, carbonylcyanide *m*-chlorophenylhydrazone; DNP, 2,4-dinitrophenol.

An analysis of the equivalent electrical circuit for these planar membranes containing bacteriorhodopsin yields information about the electrical transport characteristics of the proton pump.

GLOSSARY OF SYMBOLS

c Concentration of carbonylcyanide *m*-chlorophenylhydrazone (CCCP).
C_i Capacitance of the i^{th} element.
I_M Measured short-circuit current.
$\dot{I}_M$ Time derivative of I_M.
I_p Equivalent current generator for one vesicle.
I_0 Proton pump current for one vesicle.
J Light intensity.
n Average number of proton pumps in one fused vesicle.
N Number of vesicles fused to the BLM.
R_i Resistance of the i^{th} element.
q Charge on a proton.
V_b Bias voltage or the potential difference between the interior of the vesicle and either chamber.
V_c Constant that may be identified with the cutoff voltage of the equivalent current generator.
τ RC relaxation time.
λ The decay constant of the proton pump ($I_0 = q\lambda n_m$; see Fig. 10).
μ The excitation rate constant of the proton pump (see Fig. 10).

METHODS

Our experimental arrangement includes two Teflon chambers separated by a Teflon septum with a 1-mm diameter hole across which the BLM is formed. Aqueous salt solutions of 100 mM NaCl, 5 mM $CaCl_2$ (to promote vesicle fusion [10]) and 5 mM Tris-maleate buffer (pH 7.0) are present in each chamber. A glass window is present in one chamber for viewing and illuminating the membrane. Silver-silver chloride electrodes are used for electrical contact with the solutions, and are shielded from light.

The electrical circuit used to measure membrane resistance R_M, capacitance C_M, and short-circuit current I_M is illustrated in Fig. 1. High-impedance operational amplifiers (models 42L and AD 523L, Analog Devices, Inc., Norwood, Mass.) are used for current and voltage measurement. The outputs from these are fed to an analog-to-digital converter and then to a PDP-11/20 computer (Digital Equipment Corp., Maynard, Mass.) for storage and analysis. This allows measurements on a time scale ranging from 50 μs to several seconds.

The BLM was illuminated by a 150 W projection lamp through an optical system of our own design which contains Corning glass filters nos. 4–94 and 3–70 (yellow-green, Corning Glass Works, Corning, N.Y.). The maximum light intensity incident on the membrane was 20 ± 2 mW/cm^2 when measured with a calibrated photovoltaic diode (SEE 010 International Light, Inc., Newburyport, Mass.) and an electrometer (610C, Keithley Instruments, Inc., Cleveland, Ohio). The light intensity was varied by means of neutral density filters.

All experiments were performed at room temperature (22 ± 2°C). Purified egg lecithin (12) was used to form both the planar membranes and vesicles. BLM's were formed from a solution of the lipid in *n*-decane, 20 mg/ml. Purple membrane samples were a gift from Dr. Janos Lanyi of the Ames Research Center (Moffet Field, Calif.). The purple membrane sheets were incorporated into vesicles by sonication with an egg lecithin suspension for 25–30 min on ice. A probe-type sonicator (Instrumentation Associates, Inc., West Chester, Pa.) was used at the 1.0 A

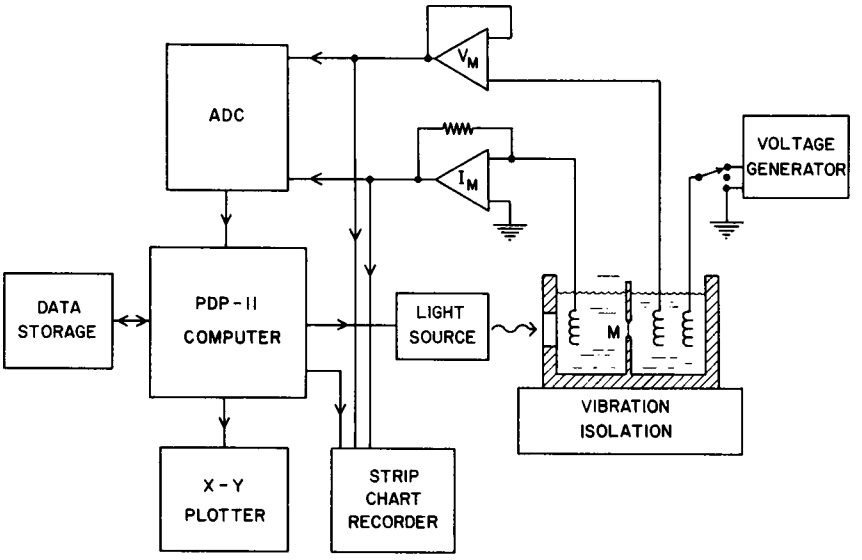

FIGURE 1 A schematic of the experimental apparatus is shown. *M* labels the planar membrane. V_M and I_M are the operational amplifiers (Analog Devices models AD523L and 42L) used to measure the membrane voltage and current.

setting. The lipid concentration was 15 mg/ml and the protein concentration was 1 mg/ml, in 100 mM NaCl, 5 mM Tris-maleate, pH 7.0.

Typically 50 μl of the vesicle suspension was added to one 20-ml chamber of the Teflon cell. The vesicles were allowed to fuse with the BLM for 4 or 5 h with stirring and were then removed by perfusion. Usually the BLM had a resistance of more than 10^{10} Ω and a capacitance of 3,000 pF before vesicles were added. After vesicle fusion, the surface of the BLM developed a silver sheen. A decrease in capacitance and increase in resistance (both by about a factor of two) was observed, presumably due to a thickening of the insulating layer separating the salt solutions.

CCCP and 2,4-dinitrophenol (DNP) were obtained from Sigma Chemical Co., St. Louis, Mo. They were dissolved in absolute ethanol and added to the aqueous solutions in this form.

RESULTS

Two qualitative observations lead us to postulate a model in which the vesicles remain intact after fusion with the planar membrane: (*a*) An increase in the short-circuit current is observed when the membrane permeability to protons is increased (see Fig. 4). (*b*) A large displacement current is observed from the planar membrane when the light is turned on (see Fig. 6). A schematic drawing of vesicles fused with a planar membrane is shown in Fig. 2 along with the equivalent electrical circuit. Each of the impedances Z_i in the equivalent circuit contains a resistor in parallel with a capacitor. All of the work presented in this paper deals with short-circuit measurements, so that Z_m may be neglected (13).

We have observed from the study of more than 30 different BLM's containing bacteriorhodopsin that the positive electrical current between the chambers is always away

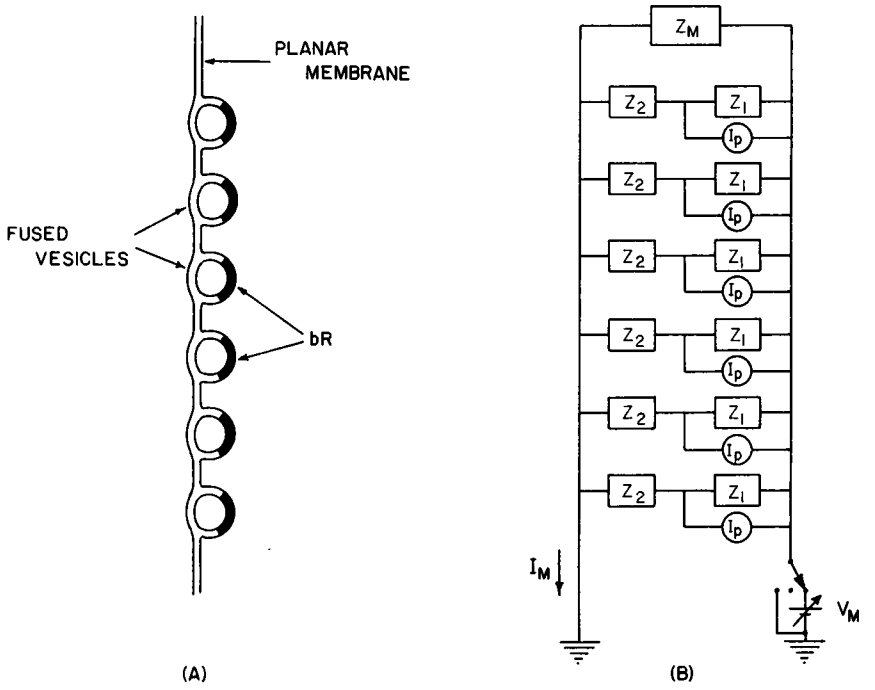

FIGURE 2 A schematic drawing of vesicles fused with a BLM is shown along with the corresponding equivalent circuit. Each of the impedances Z_i contains a resistor in parallel with a capacitor. I_M represents the membrane current and V_M is the voltage across the membrane.

from the chamber (right) to which the vesicles are added. This result indicates that the proton pumps are at least partially oriented in the BLM after fusion. The schematic drawing of a vesicle fused with a planar membrane in Fig. 3 A reflects this orientation.

R_1 and C_1 of the equivalent electrical circuit in Fig. 3 B are the resistance and capacitance between the right chamber and the interior of one vesicle. I_p is the equivalent current generator for all the proton pumps in one purple membrane sheet. R_2 and C_2 are the resistance and capacitance between the left chamber and the interior of the vesicle. V_b represents the potential difference between the interior of the vesicle and either chamber. The conservation of current at the node b requires

$$I_p(V_b,t) = V_b/R + C\,\mathrm{d}V_b/\mathrm{d}t \quad \text{with} \quad 1/R = 1/R_1 + 1/R_2 \quad \text{and} \quad C = C_1 + C_2. \tag{1}$$

Steady-State Response

The steady-state behavior ($t \to \infty$) is found by setting $C\,\mathrm{d}V_b/\mathrm{d}t = 0$. Furthermore, we assume that the equivalent current generator I_p has a linear dependence with respect to bias voltage. That is,

$$I_p(V_b,t,J) = I_0(t,J)(1 - V_b/V_c), \tag{2}$$

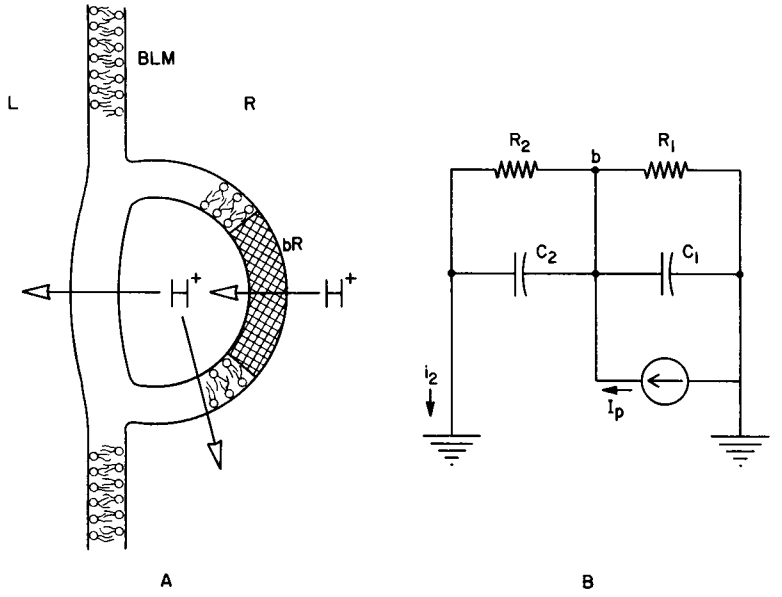

FIGURE 3 (A) A schematic drawing of a vesicle fused with a BLM is shown. BLM labels the planar membrane and the purple membrane sheet is labeled *bR*. The left chamber aqueous solution is labeled *L*, while *R* labels the right chamber. The barrier between the interior of the vesicle and the left chamber may be a multilayer. (B) The equivalent electrical circuit for a single fused vesicle is shown. R_1 and C_1 are the resistance and capacitance between the right chamber and the vesicle interior. R_2 and C_2 refer to the left side of the fused vesicle. I_p is the current generator equivalent of the proton pump.

where I_0 is the proton pump current and depends on the light intensity J, but not on V_b. V_c is a constant. This linear variation may be valid only when V_b is small compared to V_c. The node equation then becomes $I_0 = V_b(1/R + I_0/V_c)$. The current i_2 flowing through R_2 is given by V_b/R_2 and the measured short-circuit current is $I_M = Ni_2$ where N is the number of fused vesicles. Combining these equations we obtain:

$$1/I_M = R_2/NI_0R + R_2/NV_c. \tag{3}$$

The magnitude of the short-circuit steady-state current generated by a BLM containing bacteriorhodopsin under illumination *increased* when DNP or CCCP was added to reduce the membrane resistance.

Both DNP (14) and CCCP (15, 16) specifically increase the membrane permeability to protons but not to other ions. The effect of CCCP as a proton translocater has been studied in detail (16). CCCP can be used at a convenient value of pH 7.0 and was therefore chosen for our more thorough quantitative measurements.

According to Le Blanc (16), the variation of bilayer resistance with CCCP concentration may be written $1/R = 1/R_0 + ac$, where R_0 is the background resistance, a is a constant dependent on the geometry, and c is the molar CCCP concentration. This implies that at moderate CCCP concentrations R_2/R is independent of CCCP concentra-

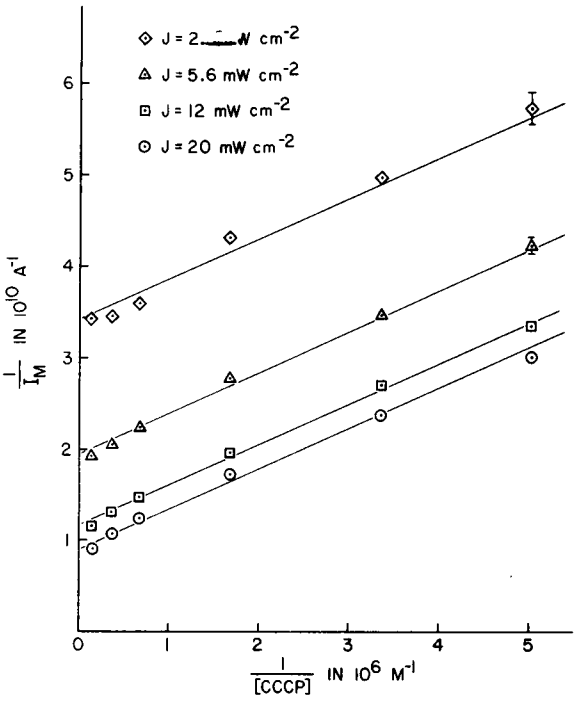

FIGURE 4 The reciprocal of the steady-state short-circuit current ($1/I_M$) generated by a BLM containing bacteriorhodopsin during illumination is shown as a function of the reciprocal of the CCCP concentration for four different light intensities.

tion and R_2 is inversely proportional to c. Therefore Eq. 3, derived from the equivalent circuit in Fig. 3 B, predicts that a plot of $1/I_M$ versus $1/c$ should be linear with a positive (light-dependent) intercept. Fig. 4 shows this predicted linear behavior when the bilayer resistance is lowered by adding CCCP to the chambers.

The rate I_0 at which the bacteriorhodopsin pumps protons should depend on light intensity J. The data presented in Fig. 5 show a linear behavior when $1/I_M$ is plotted versus $1/J$. That is,

$$1/I_M(t \rightarrow \infty) = K_1 + K_2/J. \tag{4}$$

Eq. 4 follows from Eq. 3 if $1/I_0$ is proportional to $1/J$.

Transient Response

Fig. 6 shows the transient short-circuit current from a BLM containing vesicles incorporated by vesicle fusion. The basic shape of this transient response curve follows from Fig. 3. When the light is turned on, protons are pumped to the interior of the fused vesicle and the potential at the node b increases. The measured short-circuit current consists of two contributions: a leakage current through R_2 and a displacement current through C_2. As the potential of node b approaches its steady-state value, the displacement current dies away, leaving only the steady-state current for I_M. When the

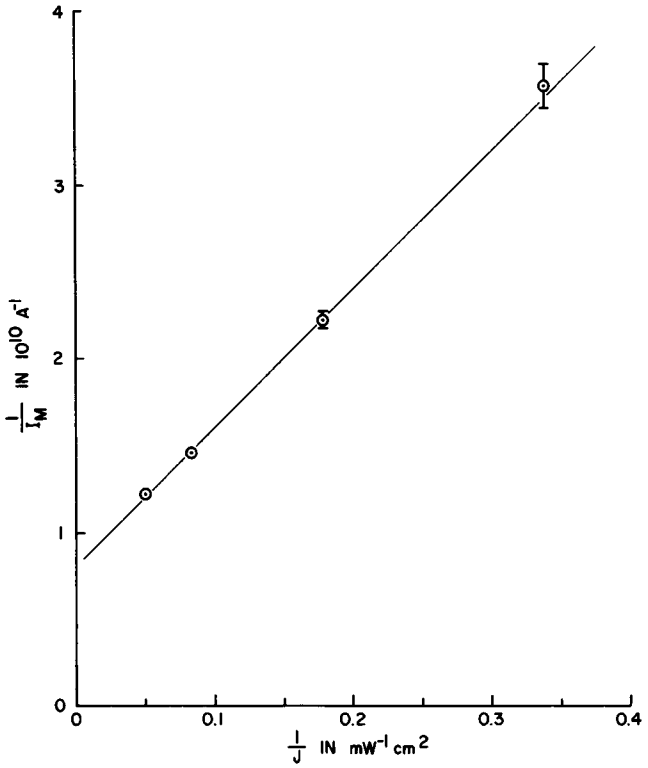

FIGURE 5 The reciprocal of the steady-state short-circuit current ($1/I_M$) generated by a BLM containing bacteriorhodopsin during illumination is shown as a function of the reciprocal of the light intensity ($1/J$). The CCCP concentration is 1.5 μM.

light is turned off, the displacement current again appears but is now of the opposite sign from the leakage current because the potential at node b is decreasing. Therefore, if the displacement current is larger than the leakage current, the short-circuit current I_M reverses sign and slowly decays to zero.

Again using conservation of current at the node b of the equivalent circuit in Fig. 3 (Eq. 1) and a linear cutoff for the equivalent current generator (Eq. 2), we have $I_0 = V_b(1/R + I_0/V_c) + C\mathrm{d}V_b/\mathrm{d}t$. The gross features associated with Fig. 6 depend on the capacitative charging and discharging of the fused vesicles. The transient response of the light-driven proton pump to a unit step of light is taken to be instantaneous on the time scale of Fig. 6.

The light is turned on at $t = 0$ and off at $t = t_0$. Therefore, we take $I_0(t) = 0$ for $t < 0$; $I_0(t) = I_0$ for $0 \leq t \leq t_0$; and $I_0(t) = 0$ for $t > t_0$. If this time dependence for $I_0(t)$ is inserted into the node equation, a differential equation for $V_b(t)$ results, which is easily solved: $V_b(t) = I_0R'(1 - e^{-t/\tau'})$, where $1/R' = 1/R + I_0/V_c$ and $\tau' = R'C$. Since $i_2 = V_b/R_2 + C_2\mathrm{d}V_b/\mathrm{d}t$ we have:

$$I_m = Ni_2 = NI_0(C_2/C)[A + Be^{-t/\tau'}] \quad 0 \leq t \leq t_0, \tag{5}$$

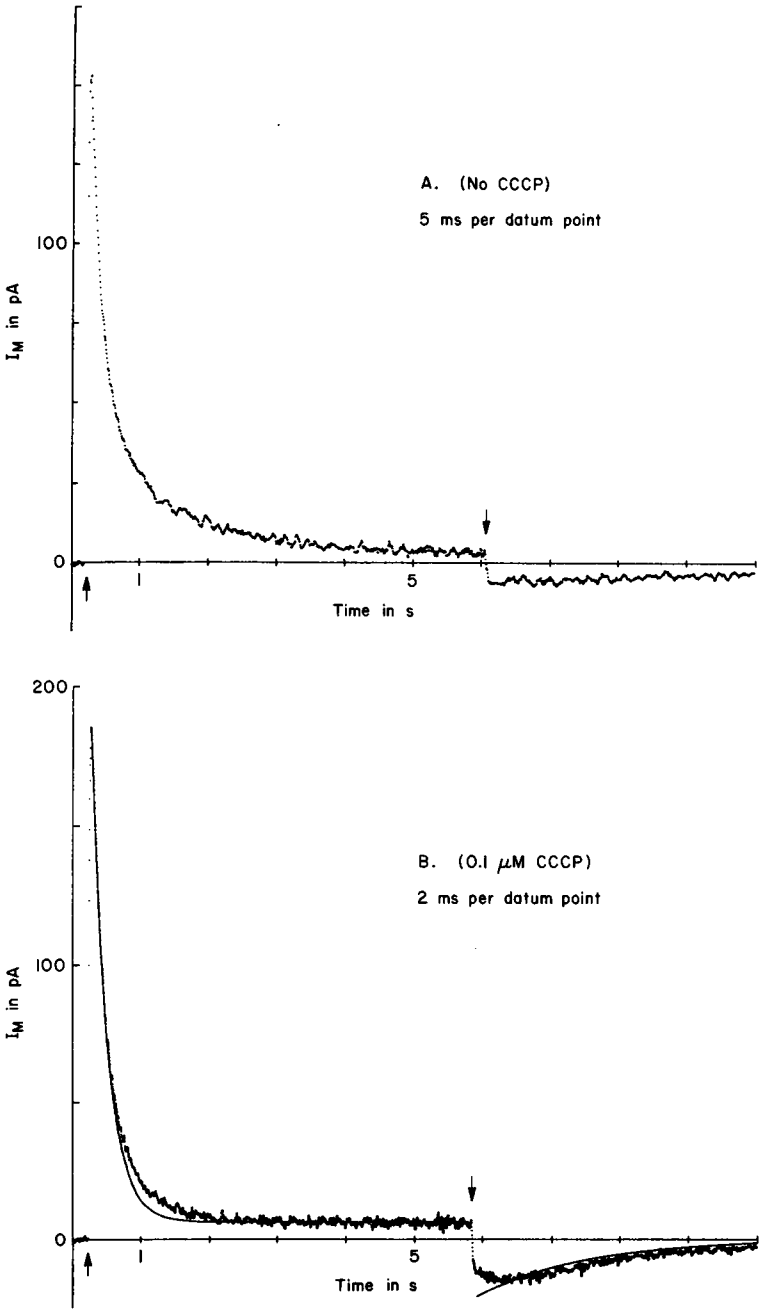

FIGURE 6 The transient short-circuit current from a BLM containing vesicles incorporated by vesicle fusion is shown. The light is turned on at the up arrow (↑) and off at the down arrow (↓). Curve 6A is without CCCP and curve 6B is with a CCCP concentration of 0.1 μM. The solid line in 6B comes from Eqs. 5 and 6. The deviation from the predicted exponential of Eq. 5 may occur because Eq. 2 is invalid at high values of V_b.

where $A = \tau'/\tau_2$, $\tau_2 = R_2C_2$, and $B = 1 - A$.

The light is turned off at $t = t_0$. The differential equation for V_b becomes $V_b/R + C\mathrm{d}V_b/\mathrm{d}t = 0$ with the solution $V_b = V^0e^{-t/RC}$ where $V^0 = V_b(t = t_0)$. It follows that $i_2 = V^0(1/R_2 - C_2/RC)e^{-t/RC}$ and we have

$$I_M = Ni_2 = (NV^0/R_2)(1 - \tau_2/\tau)e^{-t/\tau}, \quad t > t_0 \tag{6}$$

with $\tau = RC$ and $\tau_2 = R_2C_2$.

The solid curve shown in Fig. 6 B is derived from Eqs. (5) and (6) so that the potential of the node b, V_b, is continuous during the light-on–light-off cycle. The values of $\tau' = 185$ ms, $\tau = 1.25$ s, and $\tau_2 = 5.5$ s are chosen for a best fit to the data. τ' is determined from the rate of decay of the charging current. The ratio of the peak charging current to the steady-state current determines τ_2, and τ is determined from the rate of decay of the discharging current. The peak discharging current is then determined by the values of τ', τ, and τ_2.

At very low light intensities I_0 should be proportional to J. Since by definition $1/\tau' = 1/RC + I_0/CV_c$, a plot of $1/\tau'$ versus J should be linear at low light intensities. High light intensities should saturate the light-driven proton pump (I_0). A plot of $1/\tau'$ versus J is shown in Fig. 7 and shows saturation at high (20 mW/cm^2)

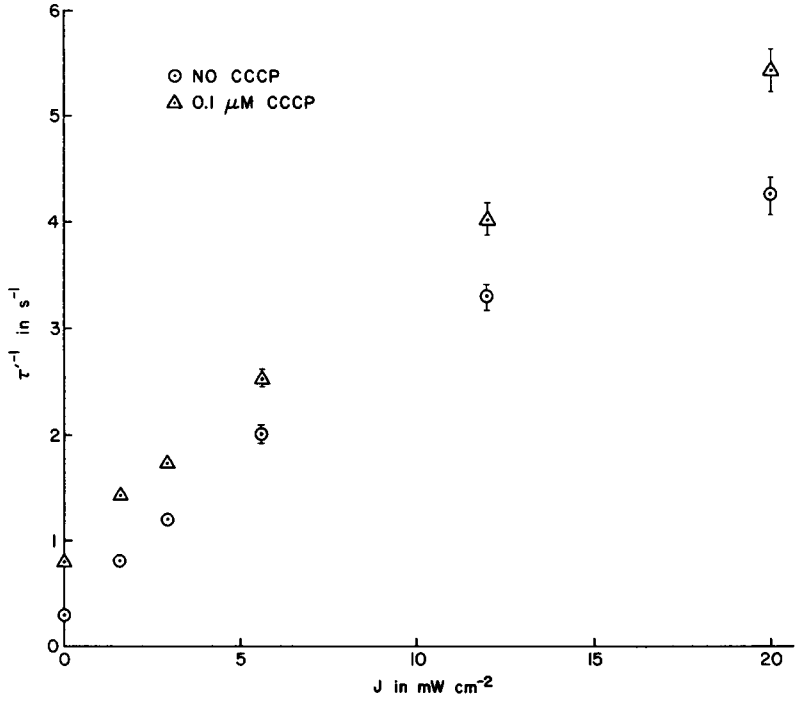

FIGURE 7 A plot of $1/\tau'$ versus light intensity J is shown. The data are for the same membrane with and without CCCP. τ' is derived from curves like those shown in Fig. 6 using Eq. 5. The saturation of τ' and therefore the light-driven proton pump (I_0) is evident.

light intensity. Therefore, due to the saturation of the light-driven proton pump at high light intensity, I_0 is not proportional to J. However, from the definition of τ and τ', we have $(1/\tau' - 1/\tau)^{-1} = CV_c/I_0$. A plot of $(1/\tau' - 1/\tau)^{-1}$ versus $1/J$ is shown in Fig. 8 and is found to be linear even at our highest light intensities; Therefore

$$1/I_0 = K_3 + K_4/J, \tag{7}$$

where K_3 and K_4 are constants.

An examination of the leading and trailing edges of the transient response curve on a much shorter time scale gives information about the transient response of the proton pump to a unit step of light. The expansion of the leading edge of Fig. 6 is shown in Fig. 9 for three different light intensities. The slope of the lines shown in the figure yield the initial slope of the short-circuit current, $\dot{I}_M(t \to 0)$, which is seen to be light dependent. A small time delay on the order of 1.5 ms is due to the time required for the electric shutter to open. The rise time of the leading edge is of order 10 ms.

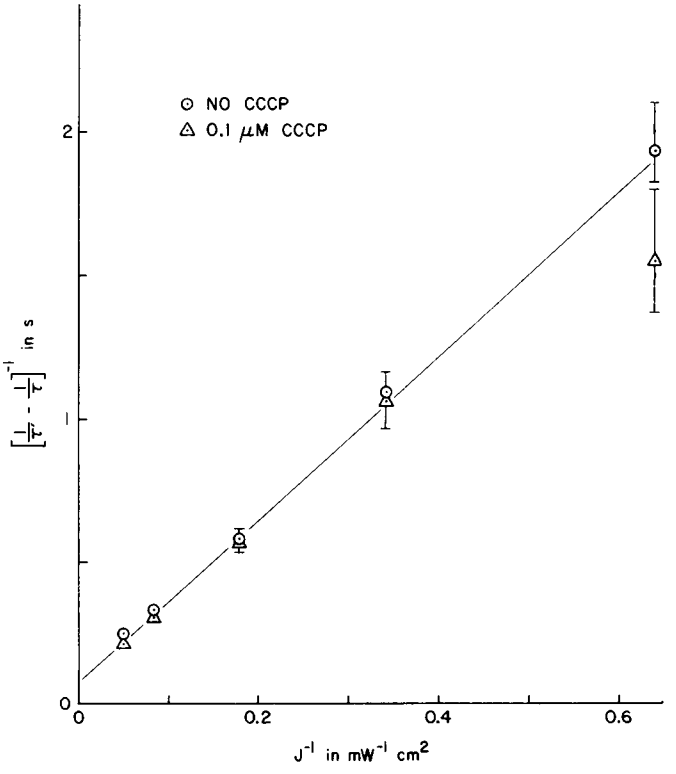

FIGURE 8 A plot of $(1/\tau' - 1/\tau)^{-1}$ versus the reciprocal of the light intensity $(1/J)$ is shown. The data is the same as that of Fig. 7. The curve is linear in spite of the saturation of the light-driven proton pump. The slope K_4 and intercept K_3 (see Eq. 7) of this curve allow a computation of ratio $\lambda/\mu J$ (see text).

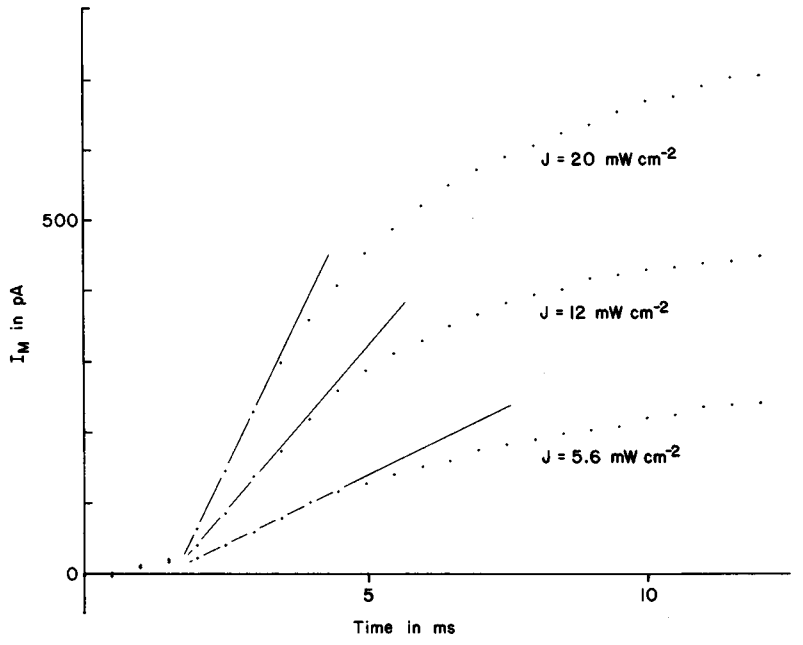

FIGURE 9 An expansion of the leading edge of the transient short-circuit current from a BLM is shown (see Fig. 6) for three different light intensities. The straight lines show the initial slope of the short-circuit current, $\dot{I}_m(t \rightarrow 0)$, when the light is turned on. The initial response of the short-circuit current is directly proportional to the initial response of the light-driven proton pump (see text).

For times less than 10 ms after the shutter is opened, V_b is small but the time rate of change of V_b is not small. Therefore we may neglect the leakage current compared to the displacement current through the capacitors C_1 and C_2.

Under these conditions the equivalent circuit of Fig. 3 reduces to that of Fig. 10 A.

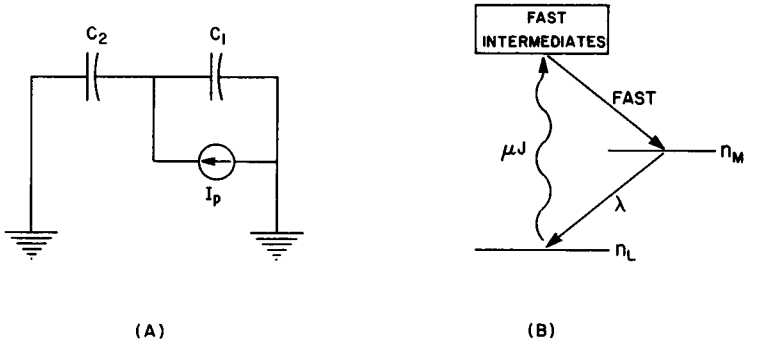

FIGURE 10 (A) The equivalent circuit for describing the planar membrane immediately after the light is turned on. (B) The cycle proposed to describe the proton pump action. Light excites the proton pump from the ground (dark) state L to an excited state M. The decay from the state M involves the translocation of protons across the membrane. μJ is the rate constant for excitation up from the ground state and λ is the rate constant for the decay from state M.

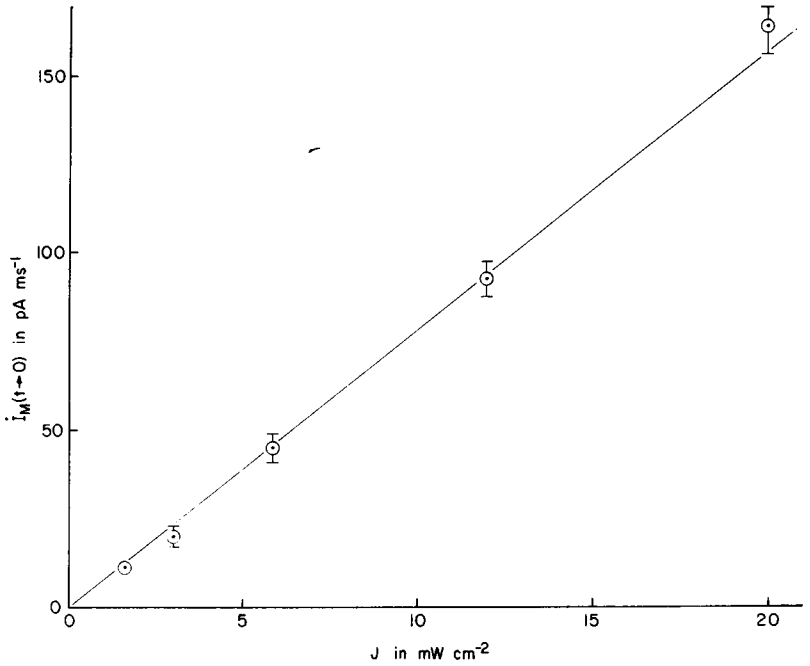

FIGURE 11 A plot of the initial slope of the short circuit current is shown as a function of the light intensity J. The result is consistent with Eq. 10 derived from the model shown schematically in Fig. 10. (see text).

Then $I_0(t) = C\mathrm{d}V_b/\mathrm{d}t$ and $i_2 = C_2\mathrm{d}V_b/\mathrm{d}t = I_0(t)\,C_2/C$. It follows that shortly after the shutter is opened we have:

$$I_M(t \to 0) = Ni_2 = N(C_2/C)I_0(t \to 0). \tag{8}$$

Thus the initial response of the short-circuit current when the shutter is opened has the same form as the initial response of the light-driven proton pump.

A plot of $\dot{I}_M(t \to 0)$ versus light intensity J, derived from curves like those shown in Fig. 9, is shown in Fig. 11. The curve is seen to be linear and passes through the origin. $\dot{I}_M(t \to 0)$ is therefore directly proportional to J. Using Eq. 8, we find that

$$\dot{I}_0 = K_5 J \tag{9}$$

where K_5 is a constant.

Varying the bilayer resistance by the addition of CCCP does not change the data shown in Fig. 11. That is, we find the initial slope of the short-circuit current $\dot{I}_M(t \to 0)$ to be independent of CCCP concentration.

DISCUSSION

The reason that the short-circuit current increases when CCCP is added to the aqueous solutions bathing the BLM follows from Fig. 3. According to Eq. 2, the equivalent

current generator depends on the potential difference between the interior of the fused vesicle and the bathing solutions. If the bilayer membrane of the system is relatively impermeable to protons, then a large potential can develop between the interior of the vesicle and the bathing solutions. This reduces the current generated by the equivalent current generator I_p. The measured short-circuit current is therefore small. Treatment with CCCP increases the permeability of the bilayer membrane, thus reducing the interior potential and allowing the current to increase. More protons escape to the left chamber (of Fig. 3 A), which results in an increase in the measured short-circuit current. A configuration in which the interior of the fused vesicle is open to the opposite chamber (11) would show no change in the short-circuit current when the BLM is treated with CCCP.

The linear dependence on bias voltage (Eq. 2) for the equivalent current generator in Fig. 3 is required for the derivation of Eq. 3. This voltage dependence of the proton pump can be interpreted as a voltage-independent current generator I_0 shunted by a resistance $R_p = V_c/I_0$ (where I_0 is light-dependent and V_c is a constant). This may reflect a light-dependent passive transport mechanism (pore) in parallel with an active proton pump. If the pore is open for a given amount of time during the photoreaction cycle, its conduction will depend on the turnover rate of the proton pump. This may account for the dependence of R_p on I_0.

Eq. 7 shows the phenomenon of saturation of the light-driven proton pump with light. An examination of the steady-state data also shows this saturation phenomenon. At very high CCCP concentration R_2 is small. Since $I_M = NV_b/R_2$, that implies V_b is very small. The value of I_M as [CCCP] $\rightarrow \infty$ is found from the intercepts of the lines in Fig. 4. Since V_b may be taken small, $I_M([\text{CCCP}] \rightarrow \infty)$ is proportional to I_0 and the light dependence of I_M reflects the light dependence of I_0. Fig. 12 shows the saturation of $I_M([\text{CCCP}] \rightarrow \infty)$ with increasing light intensity and therefore reflects the saturation of I_0.

Eq. 7 may be compared to the Michaelis-Menten equation (17), which defines the quantitative relationship between enzyme reaction rate and substrate concentration. The bacteriorhodopsin is identified as the enzyme, the number of proteins in one patch as the enzyme concentration, the photon of light is the substrate, the light intensity is the substrate concentration, the translocation of a proton is the product, and the short-circuit is the rate of velocity. This result suggests we treat the reaction as a first-order process.

We therefore make the assumption that the pump action involves essentially two states or configurations for the protein. Light excites the light-driven proton pump from a ground state L, possibly through some fast intermediates, to an excited state M. The decay from state M is associated with the translocation of protons across the membrane. This cycle is shown schematically in Fig. 10 B. Since flash spectroscopy (5–8) is associated only with the absorption properties of the chromophore in the protein, the relationship between the kinetics of the translocation of protons and the photoreaction cycle of the chromophore is not clear at this time.

We take the decay rate from state M to be λn_M, where λ is the decay constant

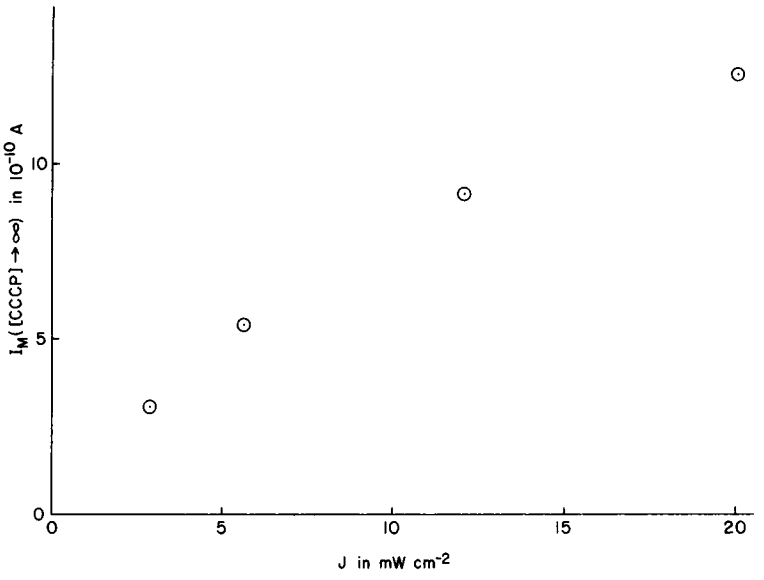

FIGURE 12 The short-circuit current extrapolated to infinite CCCP concentration $I_M([CCCP] \to \infty)$ (from Fig. 4) is shown as a function of light intensity J. The data (see text) again shows a saturation of the light-driven proton pump at our highest light intensities.

(of order 10 ms from Fig. 9) and n_M is the number of pumps in one vesicle in state M at a given time. The average rate of excitation for a single protein up from L is taken to be μJ, where μ is a constant and J is the light intensity. Therefore $dn_M/dt = \mu J n_L - \lambda n_M$. The total number of proteins in one vesicle (purple membrane sheet) is fixed: $n = n_M + n_L$. Solving the differential equation, we get $n_M(J,t) = [\mu Jn/(\mu J + \lambda)](1 - e^{-(\mu J+\lambda)t})$. The rate at which protons are moved across the membrane is λn_M: therefore the current I_0 due to the proton pumps in one vesicle becomes:

$$I_0(J,t) = q\lambda n_M(J,t) = [q\lambda\mu Jn/(\mu J + \lambda)](1 - e^{-(\mu J+\lambda)t}), \qquad (10)$$

where q is the charge of a proton. Eq. 2, used for the derivation of the equations describing the data, requires that I_0 be independent of bias voltage. Thus we expect λ to be independent of bias voltage. All of the experimental data presented in this work are consistent with the light dependence, time dependence, and voltage dependence given in Eqs. 2 and 10.

For example, from Eq. 10, $\dot{I}_0\ (t \to 0) = q\lambda\mu Jn$, in agreement with Eq. 9. Eq. 5 follows from Eq. 10 since, for the data of Fig. 8, $(\mu J + \lambda)t$ is a large quantity.

It is interesting that the ratio of λ to μJ in Fig. 10 can be found using Fig. 8 and Eq. 10. We have $(1/\tau' - 1/\tau)^{-1} = CV_c/I_0$ and from Eq. 10 $CV_c/I_0 = CV_c(\mu J + \lambda)/(q\lambda\mu Jn)$. Therefore, $(1/\tau' - 1/\tau)^{-1} = K(1 + \lambda/\mu J)$ where K is a constant. The intercept in Fig. 8 gives $K = 0.1$ s and the slope gives $K\,\lambda/\mu = 2.8$ s mW/cm^2. Thus λ/μ is 28 mW/cm^2, and at our highest light intensity $\lambda/\mu J = 1.4$. Therefore, at our highest light intensities, μJ is about 0.7 λ.

Although the leading edge of the transient response short-circuit current is essentially an exponential with respect to time (see Fig. 9), it is distorted by the development of a leakage current. The same complication enters into an analysis of the trailing edge. With the equivalent circuit of Fig. 3 and Eq. 10 it should be possible by more extensive work to get a reliable absolute value for λ.

The technical help of Mr. Malcolm Adams during the course of this work is greatly appreciated. The authors wish to thank Dr. J. Lanyi for the purple membrane samples. We also thank both Drs. J. Lanyi and R. Capaldi for a critical review of the manuscript.

This work was supported by National Science Foundation Grant DMR73-0760A01.

Received for publication 21 July 1977 and in revised form 26 September 1977.

REFERENCES

1. OESTERHELT, D., and W. STOECKENIUS. 1971. Rhodopsin-like protein from the purple membrane of *Halobacterium halobium*. *Nat. New Biol.* **233**:151.
2. DANON, A., and W. STOECKENIUS. 1974. Photophosphorylation in *Halobacterium halobium*. *Proc. Natl. Acad. Sci. U.S.A.* **71**:1234.
3. OESTERHELT, D., and W. STOECKENIUS. 1973. Functions of a new photoreceptor membrane. *Proc. Natl. Acad. Sci. U.S.A.* **70**:2853.
4. OESTERHELT, D. 1976. Bacteriorhodopsin as an example of a light-driven proton pump. *Angew. Chem. Int. Ed. Engl.* **15**:17.
5. STOECKENIUS, W., and R. H. LOZIER. 1974. Light energy conversion in *Halobacterium halobium*. *J. Supramol. Struct.* **2**:769.
6. OESTERHELT, D., and B. HESS. 1973. Reversible photolysis of the purple complex in the purple membrane of *Halobacterium halobium*. *Eur. J. Biochem.* **37**:316.
7. DENCHER, N., and M. WILMS. 1975. Flash photometric experiments on the photochemical cycle of bacteriorhodopsin. *Biophys. Struct. Mech.* **1**:259.
8. GOLDSCHMIDT, C. R., M. OTTOLENGHI, and R. KORENSTEIN. 1976. On the primary quantum yields in the bacteriorhodopsin photocycle. *Biophys. J.* **16**:839.
9. LOZIER, R. H., W. NIEDERBERGER, R. A. BOGOMOLNI, S-B. HWANG, and W. STOECKENIUS. 1976. Kinetics and stoichiometry of light-induced proton release and uptake from purple membrane fragments, *Halobacterium halobium* cell envelopes, and phospholipid vesicles containing oriented purple membrane. *Biochim. Biophys. Acta.* **440**:545.
10. DRACHEV, L. A., V. N. FROLOV, A. D. KAULEN, E. A. LIBERMAN, S. A. OSTROUMOV, V. G. PTAKUNOVA, A. Y. SEMENOV, and V. P. SKULACHEV. 1976. Reconstitution of biological molecular generators of electric current: bacteriorhodopsin. *J. Biol. Chem.* **251**:7059.
11. SHIEH, P., and L. PACKER. 1976. Photo-induced potentials across a polymer stabilized planar membrane, in the presence of bacteriorhodopsin. *Biochem. Biophys. Res. Commun.* **71**:603.
12. VREEMAN, H. J. 1966. Permeability of thin phospholipid films, Part III. *Proc. K. Akad. Wet., Ser. B. Phys. Sci.* **69**:564.
13. HERRMANN, T. R., and G. W. RAYFIELD. 1976. A measurement of the proton pump current generated by bacteriorhodopsin in black lipid membranes. *Biochem. Biophys. Acta.* **443**:623.
14. JAIN, M. K. 1972. The Biomolecular Lipid Membrane. Van Nostrand Reinhold Company, New York. 173.
15. HEYTLER, P. G. 1963. Uncoupling of oxidative phosphorylation by carbonyl cyanide hydrazones. I. Some characteristics of *m*-Cl-CCP action on mitochondria and chloroplasts. *Biochemistry.* **2**:357.
16. LE BLANC, O. H. 1971. Effect of uncouplers of oxidative phosphorylation on bilayer membranes: carbonylcyanide *m*-chlorophenylhydrazone. *J. Membrane Biol.* **4**:227.
17. See for example LENNINGER, A. L. 1972. Biochemistry. Worth Publishers, Inc., New York. 153–154.